Limits on Active to Sterile Neutrino Oscillations from Disappearance Searches in the MINOS, Daya Bay, and Bugey-3 Experiments

P. Adamson,[1,‡] F. P. An,[2,†] I. Anghel,[3,4,‡] A. Aurisano,[5,‡] A. B. Balantekin,[6,†] H. R. Band,[7,†] G. Barr,[8,‡] M. Bishai,[9,†,‡] A. Blake,[10,11,‡] S. Blyth,[12,13,†] G. J. Bock,[1,‡] D. Bogert,[1,‡] D. Cao,[14,†] G. F. Cao,[15,†] J. Cao,[15,†] S. V. Cao,[16,†] T. J. Carroll,[16,‡] C. M. Castromonte,[17,‡] W. R. Cen,[15,†] Y. L. Chan,[18,†] J. F. Chang,[15,†] L. C. Chang,[19,†] Y. Chang,[13,†] H. S. Chen,[15,†] Q. Y. Chen,[20,†] R. Chen,[21,†] S. M. Chen,[22,†] Y. Chen,[23,†] Y. X. Chen,[24,†] J. Cheng,[20,†] J.-H. Cheng,[19,†] Y. P. Cheng,[15,†] Z. K. Cheng,[25,†] J. J. Cherwinka,[6,†] S. Childress,[1,‡] M. C. Chu,[18,†] A. Chukanov,[26,†] J. A. B. Coelho,[27,‡] L. Corwin,[28,‡] D. Cronin-Hennessy,[29,‡] J. P. Cummings,[30,†] J. de Arcos,[31,†] S. De Rijck,[16,‡] Z. Y. Deng,[15,†] A. V. Devan,[32,‡] N. E. Devenish,[33,‡] X. F. Ding,[15,†] Y. Y. Ding,[15,†] M. V. Diwan,[9,†,‡] M. Dolgareva,[26,†] J. Dove,[34,†] D. A. Dwyer,[35,†] W. R. Edwards,[35,†] C. O. Escobar,[36,‡] J. J. Evans,[21,‡] E. Falk,[33,‡] G. J. Feldman,[37,‡] W. Flanagan,[16,‡] M. V. Frohne,[38,*,‡] M. Gabrielyan,[29,‡] H. R. Gallagher,[27,‡] S. Germani,[39,‡] R. Gill,[9,†] R. A. Gomes,[17,‡] M. Gonchar,[26,†] G. H. Gong,[22,†] H. Gong,[22,†] M. C. Goodman,[4,‡] P. Gouffon,[40,‡] N. Graf,[41,‡] R. Gran,[42,‡] M. Grassi,[15,†] K. Grzelak,[43,‡] W. Q. Gu,[44,†] M. Y. Guan,[15,†] L. Guo,[22,†] R. P. Guo,[15,†] X. H. Guo,[45,†] Z. Guo,[22,†] A. Habig,[42,‡] R. W. Hackenburg,[9,†] S. R. Hahn,[1,‡] R. Han,[24,†] S. Hans,[9,§,†] J. Hartnell,[33,‡] R. Hatcher,[1,‡] M. He,[15,†] K. M. Heeger,[7,†] Y. K. Heng,[15,†] A. Higuera,[46,†] A. Holin,[39,‡] Y. K. Hor,[47,†] Y. B. Hsiung,[12,†] B. Z. Hu,[12,†] T. Hu,[15,†] W. Hu,[15,†] E. C. Huang,[34,†] H. X. Huang,[48,†] J. Huang,[16,‡] X. T. Huang,[20,†] P. Huber,[47,†] W. Huo,[49,†] G. Hussain,[22,†] J. Hylen,[1,‡] G. M. Irwin,[50,‡] Z. Isvan,[9,†] D. E. Jaffe,[9,†] P. Jaffke,[47,†] C. James,[1,‡] K. L. Jen,[19,†] D. Jensen,[1,‡] S. Jetter,[15,†] X. L. Ji,[15,†] X. P. Ji,[51,22,†] J. B. Jiao,[20,†] R. A. Johnson,[5,†] J. K. de Jong,[8,‡] J. Joshi,[9,†] T. Kafka,[27,‡] L. Kang,[52,†] S. M. S. Kasahara,[29,‡] S. H. Kettell,[9,†] S. Kohn,[53,†] G. Koizumi,[1,‡] M. Kordosky,[32,‡] M. Kramer,[35,53,†] A. Kreymer,[1,‡] K. K. Kwan,[18,†] M. W. Kwok,[18,†] T. Kwok,[54,†] K. Lang,[16,‡] T. J. Langford,[7,†] K. Lau,[46,†] L. Lebanowski,[22,†] J. Lee,[35,†] J. H. C. Lee,[54,†] R. T. Lei,[52,†] R. Leitner,[55,†] J. K. C. Leung,[54,†] C. Li,[20,†] D. J. Li,[49,†] F. Li,[15,†] G. S. Li,[44,†] Q. J. Li,[15,†] S. Li,[52,†] S. C. Li,[54,47,†] W. D. Li,[15,†] X. N. Li,[15,†] Y. F. Li,[15,†] Z. B. Li,[25,†] H. Liang,[49,†] C. J. Lin,[35,†] G. L. Lin,[19,†] S. Lin,[52,†] S. K. Lin,[46,†] Y.-C. Lin,[12,†] J. J. Ling,[25,9,†,‡] J. M. Link,[47,†] P. J. Litchfield,[29,56,‡] L. Littenberg,[9,†] B. R. Littlejohn,[31,†] D. W. Liu,[46,†] J. C. Liu,[15,†] J. L. Liu,[44,†] C. W. Loh,[14,†] C. Lu,[57,†] H. Q. Lu,[15,†] J. S. Lu,[15,†] P. Lucas,[1,‡] K. B. Luk,[53,35,†] Z. Lv,[58,†] Q. M. Ma,[15,†] X. B. Ma,[24,†] X. Y. Ma,[15,†] Y. Q. Ma,[15,†] Y. Malyshkin,[59,†] W. A. Mann,[27,‡] M. L. Marshak,[29,‡] D. A. Martinez Caicedo,[31,†] N. Mayer,[27,‡] K. T. McDonald,[57,†] C. McGivern,[41,‡] R. D. McKeown,[60,32,†] M. M. Medeiros,[17,‡] R. Mehdiyev,[16,‡] J. R. Meier,[29,‡] M. D. Messier,[28,‡] W. H. Miller,[29,‡] S. R. Mishra,[61,‡] I. Mitchell,[46,†] M. Mooney,[9,†] C. D. Moore,[1,‡] L. Mualem,[60,‡] J. Musser,[28,‡] Y. Nakajima,[35,†] D. Naples,[41,‡] J. Napolitano,[62,†] D. Naumov,[26,†] E. Naumova,[26,†] J. K. Nelson,[32,‡] H. B. Newman,[60,‡] H. Y. Ngai,[54,†] R. J. Nichol,[39,‡] Z. Ning,[15,†] J. A. Nowak,[29,‡] J. O'Connor,[39,‡] J. P. Ochoa-Ricoux,[59,†] A. Olshevskiy,[26,†] M. Orchanian,[60,‡] R. B. Pahlka,[1,‡] J. Paley,[4,‡] H.-R. Pan,[12,†] J. Park,[47,†] R. B. Patterson,[60,‡] S. Patton,[35,†] G. Pawloski,[29,‡] V. Pec,[55,†] J. C. Peng,[34,†] A. Perch,[39,‡] M. M. Pfützner,[39,‡] D. D. Phan,[16,‡] S. Phan-Budd,[4,‡] L. Pinsky,[46,†] R. K. Plunkett,[1,‡] N. Poonthottathil,[1,‡] C. S. J. Pun,[54,†] F. Z. Qi,[15,†] M. Qi,[14,†] X. Qian,[9,†] X. Qiu,[50,‡] A. Radovic,[32,‡] N. Raper,[63,†] B. Rebel,[1,‡] J. Ren,[48,†] C. Rosenfeld,[61,‡] R. Rosero,[9,†] B. Roskovec,[55,†] X. C. Ruan,[48,†] H. A. Rubin,[31,‡] P. Sail,[16,‡] M. C. Sanchez,[3,4,‡] J. Schneps,[27,‡] A. Schreckenberger,[16,‡] P. Schreiner,[4,‡] R. Sharma,[1,‡] S. Moed Sher,[1,‡] A. Sousa,[5,‡] H. Steiner,[53,35,†] G. X. Sun,[15,†] J. L. Sun,[64,†] N. Tagg,[65,‡] R. L. Talaga,[4,‡] W. Tang,[9,†] D. Taychenachev,[26,†] J. Thomas,[39,‡] M. A. Thomson,[10,‡] X. Tian,[61,‡] A. Timmons,[21,‡] J. Todd,[5,‡] S. C. Tognini,[17,‡] R. Toner,[37,‡] D. Torretta,[1,‡] K. Treskov,[26,†] K. V. Tsang,[35,†] C. E. Tull,[35,†] G. Tzanakos,[66,*,‡] J. Urheim,[28,‡] P. Vahle,[32,‡] N. Viaux,[59,†] B. Viren,[9,†,‡] V. Vorobel,[55,†] C. H. Wang,[13,†] M. Wang,[20,†] N. Y. Wang,[45,†] R. G. Wang,[15,†] W. Wang,[32,25,†] X. Wang,[67,†] Y. F. Wang,[15,†] Z. Wang,[15,†] Z. M. Wang,[15,†] R. C. Webb,[68,‡] A. Weber,[8,56,‡] H. Y. Wei,[22,†] L. J. Wen,[15,†] K. Whisnant,[3,†] C. White,[31,‡] L. Whitehead,[46,†,‡] L. H. Whitehead,[39,‡] T. Wise,[6,†] S. G. Wojcicki,[50,‡] H. L. H. Wong,[53,35,†] S. C. F. Wong,[25,†] E. Worcester,[9,†] C.-H. Wu,[19,†] Q. Wu,[20,†] W. J. Wu,[15,†] D. M. Xia,[69,†] J. K. Xia,[15,†] Z. Z. Xing,[15,†] J. L. Xu,[15,†] J. Y. Xu,[18,†] Y. Xu,[25,†] T. Xue,[22,†] C. G. Yang,[15,†] H. Yang,[14,†] L. Yang,[52,†] M. S. Yang,[15,†] M. T. Yang,[20,†] M. Ye,[15,†] Z. Ye,[46,†] M. Yeh,[9,†] B. L. Young,[3,†] Z. Y. Yu,[15,†] S. Zeng,[15,†] L. Zhan,[15,†] C. Zhang,[9,†] H. H. Zhang,[25,†] J. W. Zhang,[15,†] Q. M. Zhang,[58,†] X. T. Zhang,[15,†] Y. M. Zhang,[25,†] Y. X. Zhang,[64,†] Z. J. Zhang,[52,†] Z. P. Zhang,[49,†] Z. Y. Zhang,[15,†] J. Zhao,[15,†] Q. W. Zhao,[15,†] Y. B. Zhao,[15,†] W. L. Zhong,[15,†] L. Zhou,[15,†] N. Zhou,[49,†] H. L. Zhuang,[15,†] and J. H. Zou[15,†]

[†](Daya Bay Collaboration)
[‡](MINOS Collaboration)

[1]*Fermi National Accelerator Laboratory, Batavia, Illinois 60510, USA*
[2]*Institute of Modern Physics, East China University of Science and Technology, Shanghai*
[3]*Department of Physics and Astronomy, Iowa State University, Ames, Iowa 50011 USA*
[4]*Argonne National Laboratory, Argonne, Illinois 60439, USA*
[5]*Department of Physics, University of Cincinnati, Cincinnati, Ohio 45221, USA*
[6]*Physics Department, University of Wisconsin, Madison, Wisconsin 53706, USA*
[7]*Department of Physics, Yale University, New Haven, Connecticut 06520, USA*
[8]*Subdepartment of Particle Physics, University of Oxford, Oxford OX1 3RH, United Kingdom*
[9]*Brookhaven National Laboratory, Upton, New York 11973, USA*
[10]*Cavendish Laboratory, University of Cambridge, Cambridge CB3 0HE, United Kingdom*
[11]*Lancaster University, Lancaster, LA1 4YB, United Kingdom*
[12]*Department of Physics, National Taiwan University, Taipei*
[13]*National United University, Miao-Li*
[14]*Nanjing University, Nanjing*
[15]*Institute for High Energy Physics, Protvino, Moscow Region RU-140284, Russia*
[16]*Department of Physics, University of Texas at Austin, Austin, Texas 78712, USA*
[17]*Instituto de Física, Universidade Federal de Goiás, 74690-900, Goiânia, GO, Brazil*
[18]*Chinese University of Hong Kong, Hong Kong*
[19]*Institute of Physics, National Chiao-Tung University, Hsinchu*
[20]*Shandong University, Jinan*
[21]*School of Physics and Astronomy, University of Manchester, Manchester M13 9PL, United Kingdom*
[22]*Department of Engineering Physics, Tsinghua University, Beijing*
[23]*Shenzhen University, Shenzhen*
[24]*North China Electric Power University, Beijing*
[25]*Sun Yat-Sen (Zhongshan) University, Guangzhou*
[26]*Joint Institute for Nuclear Research, Dubna, Moscow Region*
[27]*Physics Department, Tufts University, Medford, Massachusetts 02155, USA*
[28]*Indiana University, Bloomington, Indiana 47405, USA*
[29]*University of Minnesota, Minneapolis, Minnesota 55455, USA*
[30]*Siena College, Loudonville, New York 12211, USA*
[31]*Department of Physics, Illinois Institute of Technology, Chicago, Illinois 60616, USA*
[32]*Department of Physics, College of William & Mary, Williamsburg, Virginia 23187, USA*
[33]*Department of Physics and Astronomy, University of Sussex, Falmer, Brighton BN1 9QH, United Kingdom*
[34]*Department of Physics, University of Illinois at Urbana-Champaign, Urbana, Illinois 61801, USA*
[35]*Lawrence Berkeley National Laboratory, Berkeley, California, 94720 USA*
[36]*Universidade Estadual de Campinas, IFGW, CP 6165, 13083-970, Campinas, SP, Brazil*
[37]*Department of Physics, Harvard University, Cambridge, Massachusetts 02138, USA*
[38]*Holy Cross College, Notre Dame, Indiana 46556, USA*
[39]*Department of Physics and Astronomy, University College London, London WC1E 6BT, United Kingdom*
[40]*Instituto de Física, Universidade de São Paulo, CP 66318, 05315-970, São Paulo, SP, Brazil*
[41]*Department of Physics and Astronomy, University of Pittsburgh, Pittsburgh, Pennsylvania 15260, USA*
[42]*Department of Physics, University of Minnesota Duluth, Duluth, Minnesota 55812, USA*
[43]*Department of Physics, University of Warsaw, PL-02-093 Warsaw, Poland*
[44]*Department of Physics and Astronomy, Shanghai Jiao Tong University,
Shanghai Laboratory for Particle Physics and Cosmology, Shanghai*
[45]*Beijing Normal University, Beijing*
[46]*Department of Physics, University of Houston, Houston, Texas 77204, USA*
[47]*Center for Neutrino Physics, Virginia Tech, Blacksburg, Virginia 24061, USA*
[48]*China Institute of Atomic Energy, Beijing*
[49]*University of Science and Technology of China, Hefei*
[50]*Department of Physics, Stanford University, Stanford, California 94305, USA*
[51]*School of Physics, Nankai University, Tianjin*
[52]*Dongguan University of Technology, Dongguan*
[53]*Department of Physics, University of California, Berkeley, California 94720, USA*
[54]*Department of Physics, The University of Hong Kong, Pokfulam, Hong Kong*
[55]*Charles University, Faculty of Mathematics and Physics, Prague, Czech Republic*
[56]*Rutherford Appleton Laboratory, Science and Technology Facilities Council, Didcot, OX11 0QX, United Kingdom*
[57]*Joseph Henry Laboratories, Princeton University, Princeton, New Jersey 08544, USA*
[58]*Xi'an Jiaotong University, Xi'an*
[59]*Instituto de Física, Pontificia Universidad Católica de Chile, Santiago, Chile*

[60]*Lauritsen Laboratory, California Institute of Technology, Pasadena, California 91125, USA*
[61]*Department of Physics and Astronomy, University of South Carolina, Columbia, South Carolina 29208, USA*
[62]*Department of Physics, College of Science and Technology, Temple University, Philadelphia, Pennsylvania 19122, USA*
[63]*Department of Physics, Applied Physics, and Astronomy, Rensselaer Polytechnic Institute, Troy, New York 12180, USA*
[64]*China General Nuclear Power Group*
[65]*Otterbein University, Westerville, Ohio 43081, USA*
[66]*Department of Physics, University of Athens, GR-15771 Athens, Greece*
[67]*College of Electronic Science and Engineering, National University of Defense Technology, Changsha*
[68]*Physics Department, Texas A&M University, College Station, Texas 77843, USA*
[69]*Chongqing University, Chongqing*

Searches for a light sterile neutrino have been performed independently by the MINOS and the Daya Bay experiments using the muon (anti)neutrino and electron antineutrino disappearance channels, respectively. In this Letter, results from both experiments are combined with those from the Bugey-3 reactor neutrino experiment to constrain oscillations into light sterile neutrinos. The three experiments are sensitive to complementary regions of parameter space, enabling the combined analysis to probe regions allowed by the Liquid Scintillator Neutrino Detector (LSND) and MiniBooNE experiments in a minimally extended four-neutrino flavor framework. Stringent limits on $\sin^2 2\theta_{\mu e}$ are set over 6 orders of magnitude in the sterile mass-squared splitting Δm_{41}^2. The sterile-neutrino mixing phase space allowed by the LSND and MiniBooNE experiments is excluded for $\Delta m_{41}^2 < 0.8$ eV^2 at 95% CL$_s$.

The discovery of neutrino flavor oscillations [1,2] marked a crucial milestone in the history of particle physics. It indicates neutrinos undergo mixing between flavor and mass eigenstates and hence carry nonzero mass. It also represents the first evidence of physics beyond the standard model of particle physics. Since then, neutrino oscillations have been confirmed and precisely measured with data from natural (atmospheric and solar) and man-made (reactor and accelerator) neutrino sources.

The majority of neutrino oscillation data available can be well described by a three-flavor neutrino model [3–5] in agreement with precision electroweak measurements from collider experiments [6,7]. A few experimental results, however, including those from the Liquid Scintillator Neutrino Detector (LSND) [8] and MiniBooNE [9] experiments, cannot be explained by three-neutrino mixing. Both experiments observed an electron antineutrino excess in a muon antineutrino beam over short baselines, suggesting mixing with a new neutrino state with mass-squared splitting $\Delta m_{41}^2 \gg |\Delta m_{32}^2|$, where $\Delta m_{ji}^2 \equiv m_j^2 - m_i^2$, and m_i is the mass of the ith mass eigenstate. Precision electroweak measurements exclude standard couplings of this additional neutrino state for masses up to half the Z-boson mass, so that states beyond the known three active states are referred to as sterile. New light neutrino states would open a new sector in particle physics; thus, confirming or refuting these results is at the forefront of neutrino physics research.

Mixing between one or more light sterile neutrinos and the active neutrino flavors would have discernible effects on neutrino oscillation measurements. Oscillations from muon to electron (anti)neutrinos driven by a sterile neutrino require electron and muon neutrino flavors to couple to the additional neutrino mass eigenstates. Consequently, oscillations between active and sterile states will also necessarily result in the disappearance of muon (anti)neutrinos, as well as of electron (anti)neutrinos [10,11], independently of the sterile neutrino model considered [12,13].

In this Letter, we report results from a joint analysis developed in parallel to the independent sterile neutrino searches from the Daya Bay [14] and the MINOS experiments [15]. In this analysis, the measurement of muon (anti)neutrino disappearance by the MINOS experiment is combined with electron antineutrino disappearance measurements from the Daya Bay and Bugey-3 experiments [16] using the signal confidence level (CL$_s$) method [17,18]. The combined results are analyzed in light of the muon (anti)neutrino to electron (anti)neutrino appearance indications from the LSND [8] and MiniBooNE [9] experiments. The independent MINOS, Daya Bay, and Bugey-3 results are all obtained from disappearance measurements and therefore are insensitive to CP-violating effects due to mixing between the three active flavors. Under the assumption of CPT invariance, the combined results shown constrain both neutrino and antineutrino appearance.

The results reported here required several novel improvements developed independently from the Daya Bay–only [14] and MINOS-only [15] analyses, specifically, a full reanalysis of the MINOS data to search for sterile neutrino mixing, based on the CL$_s$ method, a CL$_s$-based analysis of the Bugey-3 results taking into account new reactor flux calculations and the Daya Bay experiment's reactor flux measurement, the combination of the Daya Bay results

with the Bugey-3 results taking into account correlated systematics between the experiments, and, finally, the combination of the Daya Bay + Bugey-3 and MINOS results to place stringent constraints on electron neutrino and antineutrino appearance driven by sterile neutrino oscillations.

We adopt a minimal extension of the three-flavor neutrino model by including one sterile flavor and one additional mass eigenstate. This $3 + 1$ sterile neutrino scenario is referred to as the four-flavor model in the text. In this model, the muon to electron neutrino appearance probability $P_{\nu_\mu \to \nu_e}(L/E)$ as a function of the propagation length L, divided by the neutrino energy E, can be expressed using a 4×4 unitary mixing matrix U by

$$P_{\nu_\mu \to \nu_e}(L/E) = \left| \sum_i U_{li} U_{l'i}^* e^{-i(m_i^2/2E)L} \right|^2. \quad (1)$$

In the region where $\Delta m_{41}^2 \gg |\Delta m_{32}^2|$ and for short baselines $((\Delta m_{32}^2 L/4E) \sim 0)$, Eq. (1) can be simplified to

$$P_{\nu_\mu \to \nu_e}(L/E) \approx 4|U_{e4}|^2|U_{\mu4}|^2 \sin^2\left(\frac{\Delta m_{41}^2 L}{4E}\right) \approx P_{\bar{\nu}_\mu \to \bar{\nu}_e}. \quad (2)$$

A nonzero amplitude for the appearance probability, $4|U_{e4}|^2|U_{\mu4}|^2$, is a possible explanation for the MiniBooNE and LSND results. The matrix element $|U_{e4}|^2$ can be constrained with measurements of electron antineutrino disappearance, as in the Daya Bay [14] and Bugey-3 [16] experiments. Likewise, $|U_{\mu4}|^2$ can be constrained with measurements of muon neutrino and antineutrino disappearance, as in the MINOS [15] experiment. For these experiments, the general four-neutrino survival probabilities $P_{\bar{\nu}_e \to \bar{\nu}_e}(L/E)$ and $P_{\overset{(-)}{\nu}_\mu \to \overset{(-)}{\nu}_\mu}(L/E)$ are

$$P_{\bar{\nu}_e \to \bar{\nu}_e}(L/E) = 1 - 4\sum_{k>j}|U_{ek}|^2|U_{ej}|^2 \sin^2\left(\frac{\Delta m_{kj}^2 L}{4E}\right), \quad (3)$$

$$P_{\overset{(-)}{\nu}_\mu \to \overset{(-)}{\nu}_\mu}(L/E) = 1 - 4\sum_{k>j}|U_{\mu k}|^2|U_{\mu j}|^2 \sin^2\left(\frac{\Delta m_{kj}^2 L}{4E}\right). \quad (4)$$

The mixing matrix augmented with one sterile state can be parametrized by $U = R_{34}R_{24}R_{14}R_{23}R_{13}R_{12}$ [19], where R_{ij} is the rotational matrix for the mixing angle θ_{ij}, yielding

$$|U_{e4}|^2 = \sin^2\theta_{14},$$
$$|U_{\mu4}|^2 = \sin^2\theta_{24}\cos^2\theta_{14},$$
$$4|U_{e4}|^2|U_{\mu4}|^2 = \sin^2 2\theta_{14}\sin^2\theta_{24} \equiv \sin^2 2\theta_{\mu e}. \quad (5)$$

Searches for sterile neutrinos are carried out by using the reconstructed energy spectra to look for evidence of oscillations driven by the sterile mass-squared difference Δm_{41}^2. For small values of Δm_{41}^2, corresponding to slow oscillations, the energy-dependent shape of the oscillation probability could be measured in the reconstructed energy spectra. For large values corresponding to rapid oscillations, an overall reduction in neutrino flux would be seen.

The CL_s method [17,18] is a two-hypothesis test that compares the three-flavor (null) hypothesis (labeled 3ν) to an alternate four-flavor hypothesis (labeled 4ν). To determine if the four-flavor hypothesis can be excluded, we construct the test statistic $\Delta\chi^2 = \chi_{4\nu}^2 - \chi_{3\nu}^2$, where $\chi_{4\nu}^2$ is the χ^2 value resulting from a fit to a four-flavor hypothesis, and $\chi_{3\nu}^2$ is the χ^2 value from a fit to the three-flavor hypothesis. The $\Delta\chi^2$ value observed with data, $\Delta\chi_{obs}^2$, is compared to the $\Delta\chi^2$ distributions expected if the three-flavor hypothesis is true, or the four-flavor hypothesis is true. To quantify this, we construct

$$CL_b = P(\Delta\chi^2 \geq \Delta\chi_{obs}^2 | 3\nu),$$
$$CL_{s+b} = P(\Delta\chi^2 \geq \Delta\chi_{obs}^2 | 4\nu),$$
$$CL_s = \frac{CL_{s+b}}{CL_b} \quad (6)$$

over a grid of $(\sin^2 2\theta_{14}, \Delta m_{41}^2)$ points for the Daya Bay + Bugey-3 experiments and a grid of $(\sin^2\theta_{24}, \Delta m_{41}^2)$ for the MINOS experiment. CL_b measures consistency with the three-flavor hypothesis, and CL_{s+b} measures the agreement with the four-flavor hypothesis. The alternate hypothesis is excluded at the α confidence level if $CL_s \leq 1 - \alpha$. The construction of CL_s ensures that even if CL_{s+b} is small, indicating disagreement with the four-flavor hypothesis, this hypothesis can only be excluded when CL_b is large, indicating consistency with the three-flavor hypothesis. Thus, the CL_s construction ensures the four-flavor hypothesis can only be excluded if the experiment is sensitive to it.

Calculating CL_b and CL_{s+b} can be done in two ways. The first method is the Gaussian CL_s method [20], which uses two Gaussian $\Delta\chi^2$ distributions. The first distribution is obtained by fitting toy Monte Carlo (MC) data assuming the three-flavor hypothesis is true, thus labeled as $\Delta\chi_{3\nu}^2$. The second distribution is obtained by assuming the four-flavor hypothesis is true $(\Delta\chi_{4\nu}^2)$. The mean of each distribution is obtained from a fit to the Asimov data set, an infinite statistics sample where the relevant parameters are set to best-fit values for each hypothesis [21]. The Gaussian width for the Asimov data set is derived analytically. In the second method, the distributions of $\Delta\chi^2$ are approximated by MC simulations of pseudoexperiments.

The Gaussian method is used to obtain the Daya Bay and Bugey-3 combined results, while the second method is used to obtain the MINOS results.

The MINOS experiment [22] operates two functionally equivalent detectors separated by 734 km. The detectors sample the NuMI neutrino beam [23], which yields events with an energy spectrum that peaks at about 3 GeV. Both detectors are magnetized steel and scintillator calorimeters, with the 1 kton Near Detector (ND) situated 1 km downstream of the NuMI production target, and the 5.4 kton Far Detector (FD) located at the Soudan Underground Laboratory [22]. The analysis reported here uses data from an exposure of 10.56×10^{20} protons on target, for which the neutrino beam composition is 91.8% ν_μ, 6.9% $\bar{\nu}_\mu$, and 1.3% $(\nu_e + \bar{\nu}_e)$.

To look for sterile neutrino mixing, the MINOS experiment uses the reconstructed energy spectra in the ND and FD of both charged-current (CC) and neutral-current (NC) neutrino interactions. The sterile mixing signature differs depending on the range of Δm_{41}^2 values considered. For $\Delta m_{41}^2 \in (0.005, 0.05)$ eV^2, the muon neutrino CC spectrum in the FD would display deviations from three-flavor oscillations. For rapid oscillations driven by $\Delta m_{41}^2 \in (0.05, 0.5)$ eV^2, the combination of finite detector energy resolution and rapid oscillations at the FD location would result in an apparent event rate depletion between the ND and FD. For larger sterile neutrino masses, corresponding to $\Delta m_{41}^2 > 0.5$ eV^2, oscillations into sterile neutrinos would distort the ND CC energy spectrum. Additional sensitivity is obtained by analyzing the reconstructed energy spectrum for NC candidates. The NC cross sections and interaction topologies are identical for all three active neutrino flavors, rendering the NC spectrum insensitive to standard oscillations, but mixing with a sterile neutrino state would deplete the NC energy spectrum at the FD, as the sterile neutrino would not interact in the detector. For large sterile neutrino masses, such a depletion would also be measurable at the ND.

The simulated FD-to-ND ratios of the reconstructed energy spectra for ν_μ CC and NC selected events, including four-flavor oscillations for both the ND and FD, are fit to the equivalent FD-to-ND ratios obtained from data [15]. Current and previous results of the MINOS sterile neutrino searches, along with further analysis details, are described in Refs. [15,24–26]. The MINOS experiment employs the Feldman-Cousins ordering principle [27] in obtaining exclusion limits in the four-flavor parameter space. However, this approach requires a computationally impractical joint fit to be consistent, since it requires minimizing χ^2 over Δm_{41}^2, a shared parameter between the MINOS and Daya Bay + Bugey-3 experiments. Thus, the CL$_s$ method described above is used.

While the MINOS experiment does not have any sensitivity to $\sin^2 \theta_{14}$, there is a small sensitivity to $\sin^2 \theta_{34}$ due to the inclusion of the NC channel. During
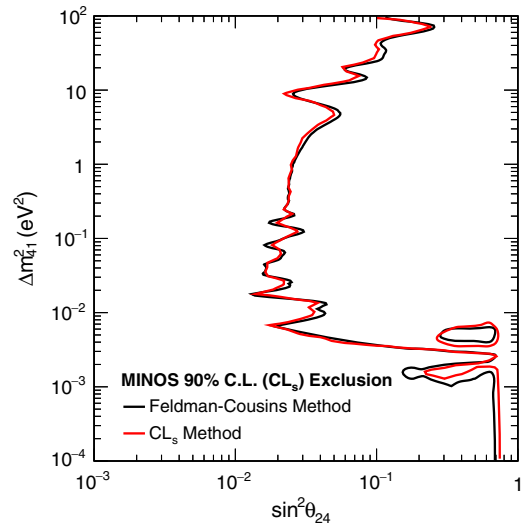

FIG. 1.   Comparison of the MINOS 90% CL contour using the Feldman-Cousins method [15] and the CL$_s$ method. The region to the right of the curve is excluded at the 90% CL (CL$_s$).

the fit, $\sin^2 \theta_{34}$ is allowed to vary freely in addition to Δm_{32}^2 and $\sin^2 \theta_{23}$, while $\sin^2 \theta_{24}$ and Δm_{41}^2 are held fixed to define the particular four-flavor hypothesis that is being tested. Since the constraint on $\sin^2 \theta_{34}$ is relatively weak, the distribution of $\Delta \chi^2$ deviates from the normal distribution and the Gaussian CL$_s$ method cannot be used. The $\Delta \chi_{3\nu}^2$ and $\Delta \chi_{4\nu}^2$ distributions are constructed by fitting pseudoexperiments.

In the three-flavor case, pseudoexperiments are simulated using the same parameters listed in Ref. [15], i.e., $\sin^2 \theta_{12} = 0.307$, $\Delta m_{21}^2 = 7.54 \times 10^{-5}$ eV^2 based on a global fit to neutrino data [28], and $\sin^2 \theta_{13} = 0.022$, based on a weighted average of results from reactor experiments [29–31]. For the atmospheric oscillation parameters, equal numbers of pseudoexperiments are simulated in the upper and lower octant ($\sin^2 \theta_{23} = 0.61$ and $\sin^2 \theta_{23} = 0.41$, respectively), with $|\Delta m_{32}^2| = 2.37 \times 10^{-3}$ eV^2, based on the most recent MINOS results [32]. The uncertainties on solar oscillation parameters have negligible effect on the analysis, so fixed values are used. In the four-flavor case, $|\Delta m_{32}^2|$, $\sin^2 \theta_{23}$, and $\sin^2 \theta_{34}$ are taken from fits to data at each $(\sin^2 \theta_{24}, \Delta m_{41}^2)$ grid point. In both the three- and four-flavor cases, half of the pseudoexperiments are generated in each mass hierarchy. A comparison of MINOS exclusion contours obtained using the Feldman-Cousins procedure [15] with those obtained using the CL$_s$ method is shown in Fig. 1. Note that if $\Delta m_{41}^2 = 2\Delta m_{31}^2$ or $\Delta m_{41}^2 \ll \Delta m_{31}^2$ and $\sin^2 \theta_{23} = \sin^2 \theta_{34} = 1$, θ_{24} can take on the role normally played by θ_{23}. In these cases, the four-flavor model is degenerate with the three-flavor model, leading to regions of parameter space that cannot be excluded.

The Daya Bay experiment measures electron antineutrinos via inverse β decay (IBD): $\bar{\nu}_e + p \to e^+ + n$.

The antineutrinos are produced by six reactor cores and detected in eight identical Gd-doped liquid-scintillator antineutrino detector (ADs) [33] in three underground experimental halls (EHs). The flux-averaged baselines for EH1, EH2, and EH3 are 520, 570, and 1590 m, respectively. The target mass in each of the two near EHs is 40 tons, and that in the far EH is 80 tons. Details of the IBD event selection, background estimates, and assessment of systematic uncertainties can be found in Refs. [29,34]. By searching for distortions in the $\bar{\nu}_e$ energy spectra, the experiment is sensitive to $\sin^2 2\theta_{14}$ for a mass-squared splitting $\Delta m_{41}^2 \in (0.0003, 0.2)$ eV^2. For $\Delta m_{41}^2 > 0.2$ eV^2, spectral distortions cannot be resolved by the detector. Instead, the measured antineutrino flux can be compared with the predicted flux to constrain the sterile neutrino parameter space. Recently, the Daya Bay Collaboration published its measurement of the overall antineutrino flux [35]. The result is consistent with previous measurements at short baselines, which prefer 5% lower values than the latest calculations [36,37], a deficit commonly referred to as the reactor antineutrino anomaly [38]. However, the reactor spectrum measurement from the Daya Bay Collaboration [35] (and from the RENO Collaboration [30] and the Double Chooz Collaboration [31]) shows clear discrepancies with the latest calculations, which indicates an underestimation of their uncertainties. The uncertainties on the antineutrino flux models for this analysis are increased to 5% from the original 2% as suggested by Refs. [39,40]. The Daya Bay Collaboration has recently updated the sterile neutrino search result in Ref. [14] with limits on $\sin^2 2\theta_{14}$ improved by about a factor of 2 with respect to previous results [41]. This data set is used in producing the combined results presented here.

Two independent sterile neutrino search analyses are conducted by the Daya Bay Collaboration. The first analysis uses the predicted $\bar{\nu}_e$ spectrum to generate the predicted prompt spectrum for each antineutrino detector simultaneously, taking into account detector effects such as energy resolution, nonlinearity, detector efficiency, and oscillation parameters described in Ref. [29]. A log-likelihood function is constructed with nuisance parameters to include the detector-related uncertainties and a covariance matrix to incorporate the uncertainties on reactor neutrino flux prediction. The Gaussian CL$_s$ method is used to calculate the excluded region. The second analysis uses the observed spectra at the near sites to predict the far site spectra to further reduce the dependency on reactor antineutrino flux models. Both analyses yield consistent results [14].

The Bugey-3 experiment was performed in the early 1990s and its main goal was to search for neutrino oscillations using reactor antineutrinos. In this experiment, two ^{6}Li-doped liquid scintillator detectors measured $\bar{\nu}_e$ generated from two reactors at three different baselines (15, 40, and 95 m) [16]. The Bugey-3 experiment detected IBD
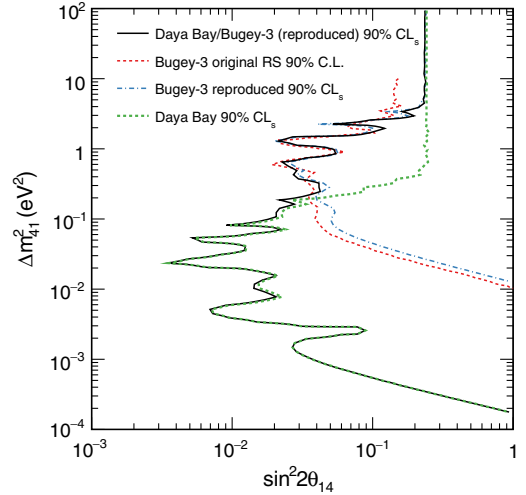

FIG. 2. Excluded regions for the original Bugey-3 raster scan (RS) result [16], for the reproduced Bugey-3 result with adjusted fluxes, for the Daya Bay result [14], and for the combined Daya Bay and reproduced Bugey-3 results. The region to the right of the curve is excluded at the 90% CL$_s$.

interactions with the recoil neutron capturing on ^{6}Li($n + {}^6$Li $\rightarrow {}^4$He $+ {}^3$H $+ 4.8$ MeV). Probing shorter baselines than the Daya Bay experiment, the Bugey-3 experiment is sensitive to regions of parameter space with larger Δm_{41}^2 values.

The original Bugey-3 results obtained using the raster scan technique are first reproduced employing a χ^2 definition used in the original Bugey-3 analysis [16]:

$$\chi^2 = \sum_i^3 \sum_j^{N_i} \frac{\{[Aa_i + b(E_j - 1.0)]R_{i,j}^{\text{pre}} - R_{i,j}^{\text{obs}}\}^2}{\sigma_{i,j}^2} + \sum_i^3 \frac{(a_i - 1)^2}{\sigma_{a_i}^2} + \frac{(A - 1)^2}{\sigma_A^2} + \frac{b^2}{\sigma_b^2}, \quad (7)$$

where A is the overall normalization, a_i is the relative detection efficiency, b is an empirical factor to include the uncertainties of the energy scale, i represents the data from three baselines, and j sums over the N_i bins at each baseline. The values of σ_{a_i} and σ_b are set at 0.014 MeV^{-1} and 0.020 MeV^{-1}, respectively, according to the reported values in Ref. [16]. The $\sigma_{i,j}$ are the statistical uncertainties. The uncertainty on the overall normalization σ_A is set to 5% to be consistent with the constraint employed in the Daya Bay analysis [14]. The ratio of the observed spectrum to the predicted unoscillated spectrum is denoted by $R_{i,j}^{\text{obs}}$, while $R_{i,j}^{\text{pre}}$ is the predicted ratio of the spectrum including oscillations to the one without oscillations. To predict the energy spectra, the average fission fractions are used [42], and the energy resolution is set to 5% at 4.2 MeV [16] with a functional form similar to the Daya Bay
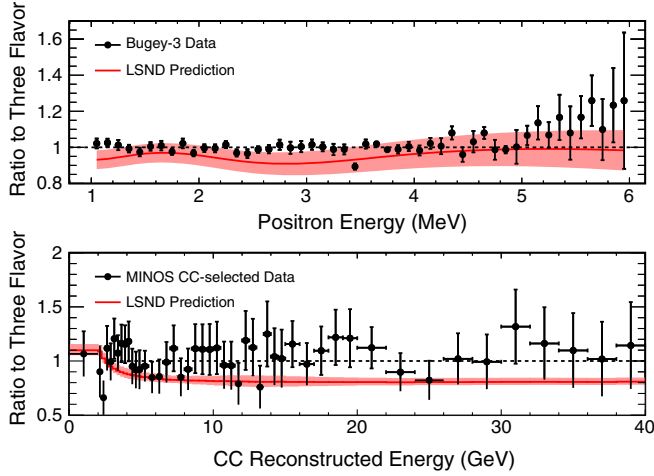
FIG. 3.   The top panel shows the ratio of the Bugey-3 15 m IBD data to a three-neutrino prediction, while the bottom panel shows the ratio of the MINOS FD-to-ND ratio data for CC events to a three-neutrino prediction. The red lines represent the four-flavor predictions at ($\Delta m_{41}^2 = 1.2$ eV^2, $\sin^2 2\theta_{\mu e} = 0.003$). The shaded band displays the sizes of the systematic uncertainties. A value of $\sin^2 2\theta_{14} = 0.11$ is used for the Bugey-3 prediction so that when multiplied by the MINOS 90% CL$_s$ limit on $\sin^2 \theta_{24}$, it matches $\sin^2 2\theta_{\mu e} = 0.003$. A $\Delta\chi^2$ value of 48.2 is found between the data and this 4ν prediction. Similarly, a value of $\sin^2 \theta_{24} = 0.12$ is combined with the Bugey-3 90% CL$_s$ limit on θ_{14} to produce the MINOS four-flavor prediction, resulting in $\Delta\chi^2 = 38.0$ between the data and the prediction.

experiment's. The predicted energy spectra are validated against the published Bugey-3 spectra [16].

In the Bugey-3 experiment, the change in the oscillation probability over the baselines of the detectors and the reactors is studied with MC simulations assuming that antineutrinos are uniformly generated in the reactor cores and uniformly measured in the detectors, and approximated by treating the baselines as normal distributions. To achieve the combination with the Daya Bay experiment, two changes are made in the reproduced Bugey-3 analysis: the change in the cross section of the IBD process due to the updated neutron decay time [6] is applied, and the anti-neutrino flux is adjusted from the ILL + Vogel model [43,44] to that of Huber [36] and Mueller [37], for consistency with the prediction used by the Daya Bay experiment. These adjustments change the reproduced contour with respect to the original Bugey-3 one, in particular by reducing the sensitivity to regions with $\Delta m_{41}^2 > 3$ eV^2, with less noticeable effects for smaller Δm_{41}^2 values. The reproduced Bugey-3 limit on the sterile neutrino mixing, and the limit obtained by combining the Bugey-3 with the Daya Bay results through a χ^2 fit, with common overall normalization and oscillation parameters, are shown in Fig. 2.

Individually, the MINOS and Bugey-3 experiments are both sensitive to regions of parameter space allowed by the
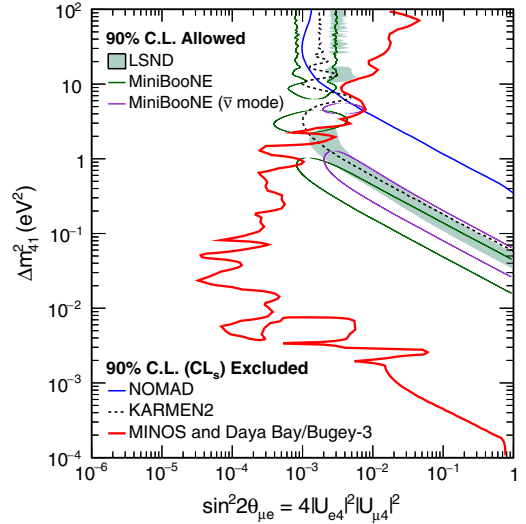

FIG. 4.   MINOS and Daya Bay + Bugey-3 combined 90% CL$_s$ limit on $\sin^2 2\theta_{\mu e}$ compared to the LSND and MiniBooNE 90% CL allowed regions. Regions of parameter space to the right of the red contour are excluded. The regions excluded at 90% CL by the KARMEN2 Collaboration [45] and the NOMAD Collaboration [46] are also shown. We note that the excursion to small mixing in the exclusion contour at around $\Delta m_{41}^2 \sim 5 \times 10^{-3}$ eV^2 is originated from the island in Fig. 1.

LSND measurement through constraints on θ_{24} and θ_{14}, shown in Figs. 1 and 2, respectively. We illustrate this sensitivity in Fig. 3, which displays a comparison of the energy spectra for the Bugey-3 and MINOS data to four-flavor (4ν) predictions produced at the LSND best-fit point [8] as an example. For the Bugey-3 experiment, a $\Delta\chi^2$ value of 48.2 is found between the data and the four-flavor prediction. Taking equal priors between these two models, the posterior likelihood for 3ν vs 4ν is 1 vs 3.4×10^{-11} in the Bayesian framework. For the MINOS experiment, a $\Delta\chi^2$ value of 38.0 is obtained between data and prediction. The posterior likelihood for 3ν vs 4ν is 1 vs 5.6×10^{-9}.

In our combined analysis, we obtain $\Delta\chi^2_{\rm obs}$ as well as $\Delta\chi^2_{3\nu}$ and $\Delta\chi^2_{4\nu}$ distributions for each ($\sin^2 2\theta_{14}$, Δm_{41}^2) grid point of the Daya Bay and Bugey-3 combination, and for each ($\sin^2 \theta_{24}$, Δm_{41}^2) grid point from the MINOS experiment. We then combine pairs of grid points from the MINOS and the Daya Bay and Bugey-3 results at fixed values of Δm_{41}^2 to obtain constraints on electron neutrino or antineutrino appearance due to oscillations into sterile neutrinos. Since the systematic uncertainties of accelerator and reactor experiments are largely uncorrelated, for each ($\sin^2 2\theta_{14}$, $\sin^2 \theta_{24}$, Δm_{41}^2) grid point, a combined $\Delta\chi^2_{\rm obs}$ is constructed from the sum of the corresponding MINOS and Daya Bay + Bugey-3 $\Delta\chi^2_{\rm obs}$ values. Similarly, the combined $\Delta\chi^2_{3\nu}$ and $\Delta\chi^2_{4\nu}$ distributions are constructed by adding random samples drawn from the corresponding MINOS and Daya Bay + Bugey-3 distributions. Finally,

the CL_s value at every $(\sin^2 2\theta_{14}, \sin^2\theta_{24})$ point is calculated using Eq. (6), while the Δm_{41}^2 value is fixed. While CL_s is single valued at every $(\sin^2 2\theta_{14}, \sin^2\theta_{24})$ point for a given value of Δm_{41}^2, it is multivalued as a function of $\sin^2 2\theta_{\mu e}$ [cf. Eq. (5)]. To obtain a single-valued function, we make the conservative choice of selecting the largest CL_s value for any given $\sin^2 2\theta_{\mu e}$. The 90% CL_s exclusion contour resulting from this procedure is shown in Fig. 4. Under the assumption of *CPT* conservation, the combined constraints are equally valid in constraining electron neutrino or antineutrino appearance. The combined results of the Daya Bay + Bugey-3 and MINOS experiments constrain $\sin^2 2\theta_{\mu e} < [3.0 \times 10^{-4} \ (90\% \ CL_s), 4.5 \times 10^{-4} \ (95\% \ CL_s)]$ for $\Delta m_{41}^2 = 1.2 \ \text{eV}^2$.

In conclusion, we have combined constraints on $\sin^2 2\theta_{14}$ derived from a search for electron antineutrino disappearance at the Daya Bay and Bugey-3 reactor experiments with constraints on $\sin^2\theta_{24}$ derived from a search for muon (anti)neutrino disappearance in the NuMI beam at the MINOS experiment. Assuming a four-flavor model of active-sterile oscillations, we constrain $\sin^2 2\theta_{\mu e}$, the parameter controlling electron (anti)neutrino appearance at short-baseline experiments, over 6 orders of magnitude in Δm_{41}^2. We set the strongest constraint to date and exclude the sterile neutrino mixing phase space allowed by the LSND and MiniBooNE experiments for $\Delta m_{41}^2 < 0.8 \ \text{eV}^2$ at a 95% CL_s. Our results are in good agreement with results from global fits (see Refs. [13,47] and references therein) at specific parameter choices; however, they differ in detail over the range of parameter space. The results explicitly show the strong tension between null results from disappearance searches and appearance-based indications for the existence of light sterile neutrinos.

Note added.—Recently, a paper appeared by the IceCube Collaboration that sets limits using sterile-driven disappearance of muon neutrinos [48]. The results place strong constraints on $\sin^2 2\theta_{24}$ for $\Delta m_{41}^2 \in (0.1, 10) \ \text{eV}^2$. Further, a paper that reanalyses the same IceCube data in a model including nonstandard neutrino interactions also appeared [49].

*Deceased.

§Present address: Department of Chemistry and Chemical Technology, Bronx Community College, Bronx, New York 10453, USA.

[1] Y. Fukuda *et al.* (Super-Kamiokande Collaboration), Phys. Rev. Lett. **81**, 1562 (1998).

[2] Q. R. Ahmad *et al.* (SNO Collaboration), Phys. Rev. Lett. **87**, 071301 (2001).

[3] B. Pontecorvo, Sov. Phys. JETP **6**, 429 (1957).

[4] B. Pontecorvo, Sov. Phys. JETP **26**, 984 (1968).

[5] Z. Maki, M. Nakagawa, and S. Sakata, Prog. Theor. Phys. **28**, 870 (1962).

[6] K. Olive *et al.* (Particle Data Group), Chin. Phys. C **38**, 090001 (2014).

[7] S. Schael (ALEPH Collaboration, DELPHI Collaboration, L3 Collaboration, OPAL Collaboration, SLD Collaboration, LEP Electroweak Working Group, SLD Electroweak Group, SLD Heavy Flavour Group), Phys. Rep. **427**, 257 (2006).

[8] A. Aguilar *et al.* (LSND Collaboration), Phys. Rev. D **64**, 112007 (2001).

[9] A. Aguilar-Arevalo *et al.* (MiniBooNE Collaboration), Phys. Rev. Lett. **110**, 161801 (2013).

[10] N. Okada and O. Yasuda, Int. J. Mod. Phys. A **12**, 3669 (1997).

[11] S. M. Bilenky, C. Giunti, and W. Grimus, Eur. Phys. J. C **1**, 247 (1998).

[12] C. Giunti and E. M. Zavanin, Mod. Phys. Lett. A **31**, 1650003 (2016).

[13] J. Kopp, P. A. N. Machado, M. Maltoni, and T. Schwetz, J. High Energy Phys. 05 (2013) 050.

[14] F. P. An *et al.* (Daya Bay Collaboration), following Letter, Phys. Rev. Lett. **117**, 151802 (2016).

[15] P. Adamson *et al.* (MINOS Collaboration), this issue, Phys. Rev. Lett. **117**, 151803 (2016).

[16] B. Achkar *et al.*, Nucl. Phys. **B434**, 503 (1995).

[17] A. L. Read, J. Phys. G **28**, 2693 (2002).

[18] T. Junk, Nucl. Instrum. Methods Phys. Res., Sect. A **434**, 435 (1999).

[19] H. Harari and M. Leurer, Phys. Lett. B **181**, 123 (1986).

[20] X. Qian, A. Tan, J. J. Ling, Y. Nakajima, and C. Zhang, Nucl. Instrum. Methods Phys. Res., Sect. A **827**, 63 (2016).

[21] G. Cowan, K. Cranmer, E. Gross, and O. Vitells, Eur. Phys. J. C **71**, 1 (2011); **73**, 2501(E) (2013).

[22] D. G. Michael *et al.* (MINOS Collaboration), Nucl. Instrum. Methods Phys. Res., Sect. A **596**, 190 (2008).

[23] P. Adamson *et al.* (MINOS Collaboration), Nucl. Instrum. Methods Phys. Res., Sect. A **806**, 279 (2016).

[24] P. Adamson *et al.* (MINOS Collaboration), Phys. Rev. Lett. **107**, 011802 (2011).

[25] P. Adamson *et al.* (MINOS Collaboration), Phys. Rev. D **81**, 052004 (2010).

[26] P. Adamson *et al.* (MINOS Collaboration), Phys. Rev. Lett. **101**, 221804 (2008).

[27] G. J. Feldman and R. D. Cousins, Phys. Rev. D **57**, 3873 (1998).

[28] G. L. Fogli, E. Lisi, A. Marrone, D. Montanino, A. Palazzo, and A. M. Rotunno, Phys. Rev. D **86**, 013012 (2012).

[29] F. P. An *et al.*, Phys. Rev. Lett. **115**, 111802 (2015).

[30] J. H. Choi *et al.* (RENO Collaboration), Phys. Rev. Lett. **116**, 211801 (2016).

[31] Y. Abe *et al.* (Double Chooz Collaboration), J. High Energy Phys. 10 (2014) 086; 02 (2015) 74.

[32] P. Adamson *et al.* (MINOS Collaboration), Phys. Rev. Lett. **112**, 191801 (2014).

[33] F. P. An *et al.* (Daya Bay Collaboration), Nucl. Instrum. Methods Phys. Res., Sect. A **811**, 133 (2016).

[34] F. An *et al.* (Daya Bay Collaboration), Phys. Rev. Lett. **112**, 061801 (2014).

[35] F. P. An *et al.* (Daya Bay Collaboration), Phys. Rev. Lett. **116**, 061801 (2016).

[36] P. Huber, Phys. Rev. C **84**, 024617 (2011); **85**, 029901(E) (2012).

[37] T. A. Mueller, D. Lhuillier, M. Fallot, A. Letourneau, S. Cormon, M. Fechner, L. Giot, T. Lasserre, J. Martino, G. Mention, A. Porta, and F. Yermia, Phys. Rev. C **83**, 054615 (2011).

[38] G. Mention, M. Fechner, T. Lasserre, T. A. Mueller, D. Lhuillier, M. Cribier, and A. Letourneau, Phys. Rev. D **83**, 073006 (2011).

[39] A. C. Hayes, J. L. Friar, G. T. Garvey, G. Jungman, and G. Jonkmans, Phys. Rev. Lett. **112**, 202501 (2014).

[40] P. Vogel, arXiv:1603.08990.

[41] F. An *et al.*, Phys. Rev. Lett. **113**, 141802 (2014).

[42] Y. Declais *et al.*, Phys. Lett. B **338**, 383 (1994).

[43] K. Schreckenbach, G. Colvin, W. Gelletly, and F. Von Feilitzsch, Phys. Lett. B **160**, 325 (1985).

[44] P. Vogel, Phys. Rev. D **29**, 1918 (1984).

[45] B. Armbruster *et al.* (KARMEN Collaboration), Phys. Rev. D **65**, 112001 (2002).

[46] P. Astier *et al.* (NOMAD Collaboration), Phys. Lett. B **570**, 19 (2003).

[47] S. Gariazzo, C. Giunti, M. Laveder, Y. F. Li, and E. M. Zavanin, J. Phys. G **43**, 033001 (2016).

[48] M. G. Aartsen *et al.* (IceCube Collaboration), Phys. Rev. Lett. **117**, 071801 (2016).

[49] J. Liao and D. Marfatia, Phys. Rev. Lett. **117**, 071802 (2016).